# Carbon dust in aluminum electrolysis pots - a vicious circle

**Louis Bugnion[1], Jean-Claude Fischer[2]**
1. Electrolysis Manager,
2. Director,
R&D Carbon, Sierre, Switzerland
Corresponding author: jeanclaude.fischer@rd-carbon.com

**Abstract**

Anode dusting in electrolytic bath has been known for years to deteriorate pot performance in aluminum smelters. Suspended carbon particles increase electrical resistivity of the bath, triggering a series of adverse effects for the pot. Under constant pot parameters, carbon dust originates from poor anode quality. In conjunction with faulty pot operation, high dusting level can develop into crisis which will impact production figures for several months. A few examples of crises related to carbon dust are reviewed from root causes to resolution. As a result, a methodology to monitor dusting level and quantify its effect on bath resistivity and pot stability is proposed. Based on plant data analysis and on-site measurements, it allows for comparison between pots and anode populations, making the link between anode quality and pot performance. Eventually it provides a sound basis for the prevention of crises and economical carbon management.

**Keywords:** Carbon dusting in pots; anode quality; pot performance, electrolyte resistivity.

## 1. Introduction

Carbon dust is one of the impurities present in electrolytic bath. Carbon particles have a size ranging from micron to centimetre scale with an average size between 1 and 10 µm [1, 2]. Coarse particles float at the bath surface whereas finer ones are suspended in the electrolyte. The average carbon concentration in the bath is of the order of 0.05 % and varies as a function of bath depth [2]. It is larger at the bath-metal interface and close to the bath surface where the coarse particles are found. In dusty pots, the carbon concentration in the bath can reach values as high as 0.4 % [3] with severe consequences for the pot performance.

Carbon dust mainly originates from selective burning of the anodes in contact with $CO_2$ or air. The binder matrix is burnt preferentially, loosening carbon particles into the bath or within the crust/anode cover. The combustion reactions take place at the anode surface or in the anode bulk where the gases are able to permeate. The reaction rates depend on the temperature, surface structure, permeability and reactivity of the anodes constituents [4].

Other sources of carbon dust are identified such as cathode and ramming paste wear. Carbon fines entrained by the fumes and captured by the dry scrubber system return to the pot through secondary alumina feeding. Likewise, recycled anode cover contains carbon particles which contaminate the bath when falling into it.

The cycle of carbon dust in the electrolytic bath is complex and mechanisms of generation of fine particles, combustion rate and accumulation patterns of suspended particles, impact on bath properties are poorly understood. Carbon excess consumption figures give a hint about the total amount of anode carbon which is not used for the electrochemical reactions but fall short on predicting how much, where and for how long carbon dust remains in the bath.

Over the years, strategies were developed with the objective of 1) Preventing the formation of carbon dust, 2) Monitoring the carbon concentration in the bath and 3) Removing carbon dust from the electrolyte.

1) Major efforts were made in the production of anodes to limit their propensity to dusting [5]. Concurrently, laboratory tests were developed allowing qualifying anodes. $CO_2$ and air reactivity, air permeability and concentrations of the elements S, V, Na and Ca are the most relevant anode properties with regard to dusting. Routine measurements are mandatory to assess anode quality and to detect issues in the manufacturing process.

   From the pot operation and pot design point of view, bath temperature, anode temperature, anode cover, anode cycle time, current density, anode balance, collar stud protection, butts height play an important role in the accumulation of carbon dust. Monitoring of the parameters and optimization based on cost-benefit ratio shall be realized. However, as discussed below, the cost of carbon dust is always difficult to assess.

2) The carbon concentration in the electrolyte can be measured directly from bath samples or indirectly from samples of secondary alumina, recycled anode cover or skimmed material. Visual observation of anode cover and bath surface and a simple rating system can also be used to monitor dusting level in pots [6]. In the following, a comprehensive method to quantify carbon concentration and its effect on bath resistivity and anode-cathode distance (ACD) is presented.

3) Carbon dust in bath is naturally removed by burning. Skimming at the taphole or cleaning of the anode cavity during anode change are necessary measures to further reduce dusting level.

## 2. Impact on pot performance

The primary effect of carbon dust is to increase the bath electrical resistivity. Since the cell voltage is prescribed by the process control, a higher dusting level will result in an ACD squeeze. Even though the dependence of bath resistivity on carbon concentration and granulometry is little documented [7], the causal relationship is well known and is the starting point for a chain reaction of adverse effects illustrated in Figure 1. A lower ACD will affect pot stability and current efficiency [8], increasing bath temperature. As a result, the cell performance is reduced and the propensity to dusting is enhanced.

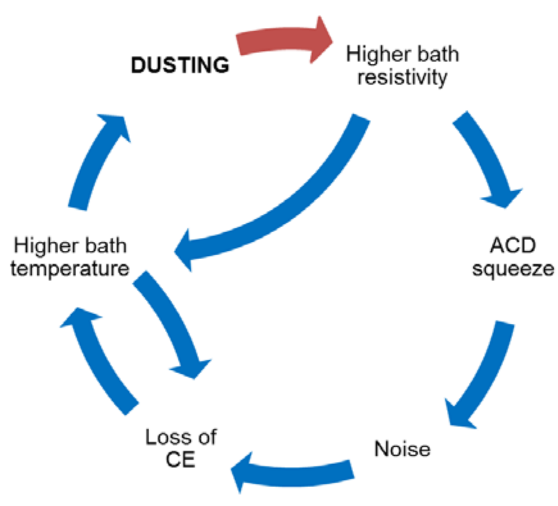


**Figure 1. Vicious circle triggered by anode dusting.**

In order to assess the impact of carbon dust on bath resistivity and on the resulting ACD squeeze, a simple method is applied. The beam is moved downwards by a few mm and it is kept at that very position during 10 min until it is moved downwards again. The cell voltage and beam position are recorded as a function of time. The test is stopped when the pot starts to oscillate. In order to improve precision and to assess the reproducibility of the measurement, the same operation can be repeated with upwards beam displacements. Cell voltage and beam position yield following quantities: 1) The increase of noise level as a function of ACD decrease and 2) The variation of pot voltage per mm of modified ACD. 1) Provides information on the stability margin of the pot whereas, 2) Quantifies the bath electrical resistivity. The test was performed on two groups of pots in one potline: a first group composed of four clean pots and a second group with two dusty pots. Carbon content of bath samples from all 6 pots was determined using Leco method and XRF as control (see Table 1). The average carbon content was equal to 0.07 % for the clean pots and 0.11 % for the dusty pots. In Figure 2, the voltage of one pot from each group is plotted versus time during the downwards beam movements.

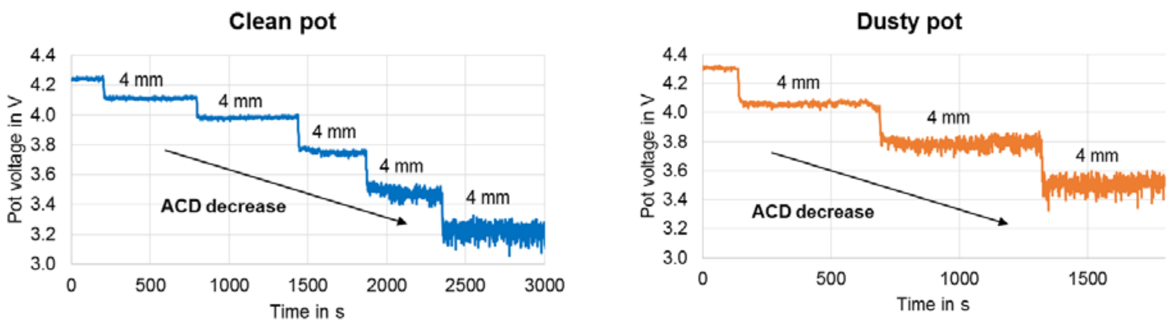


**Figure 2. Pot voltage versus time during ACD squeeze in a clean pot and in a dusty pot.**

One observes that the increase in noise level occurs earlier for the dusty pot. It is well visible when plotting the noise level (standard deviation of the cell voltage) as a function of the ACD decrease for the two pots (see Figure 3).

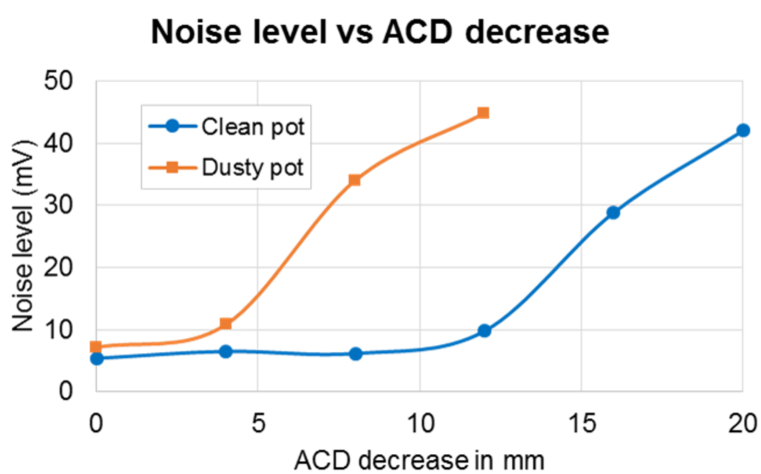


**Figure 3. Noise level versus ACD decrease during ACD squeeze in a clean pot and in a dusty pot.**

The acceptable noise level limit of 20 mV is exceeded after 6 mm of ACD decrease for the dusty pot and after 14 mm for the clean pot. Since pot design and pot operation are the same, the discrepancy is mainly explained by the fact that the initial ACD levels are not equal (the initial pot voltage values are). This is confirmed by the analysis of the variation of pot voltage per mm of modified ACD which is expected to be proportional to bath resistivity $\Delta U/\Delta ACD = \rho_{bath} \cdot I/S$ with $S$ the total anode surface (see Table 1). Only data points with noise level below 20 mV are considered □ at higher noise level, effects related to changing fanning factor and oscillations of the bath-metal interface distort the proportionality relationship □ and data points are averaged over each group of pots. From the squeeze test, one obtains that the voltage variation per mm of modified ACD is equal to 47 mV/mm for the clean pots and 61 mV/mm for dusty pots. This represents a 30 % larger bath resistivity which can be attributed to the presence of carbon dust in the electrolyte. As a comparison, the voltage variation per mm of modified ACD predicted by the bath resistivity formula [9] using the bath temperature and bath composition data is equal to 42 mV/mm and 41 mV/mm respectively.

**Table 1. Variation of pot voltage per mm of modified ACD for the two groups of pots.**

| | # pots | ΔU/ΔACD Squeeze test mV/mm | ΔU/ΔACD Bath res. formula mV/mm | Carbon content Leco % |
|---|---|---|---|---|
| Clean pots | 4 | 47 | 42 | 0.07 |
| Dusty pots | 2 | 61 | 41 | 0.11 |

It is clear that such a large difference only concerns a small number of pots. However, critical pots are revealing of the distribution of the relevant parameter within the pot population. As illustrated in Figure 4, pot parameter distributions (here current efficiency) shall have close mode values but less close mean values. Likewise, they shall behave very differently in case of enhanced stress in anode quality or pot operation.

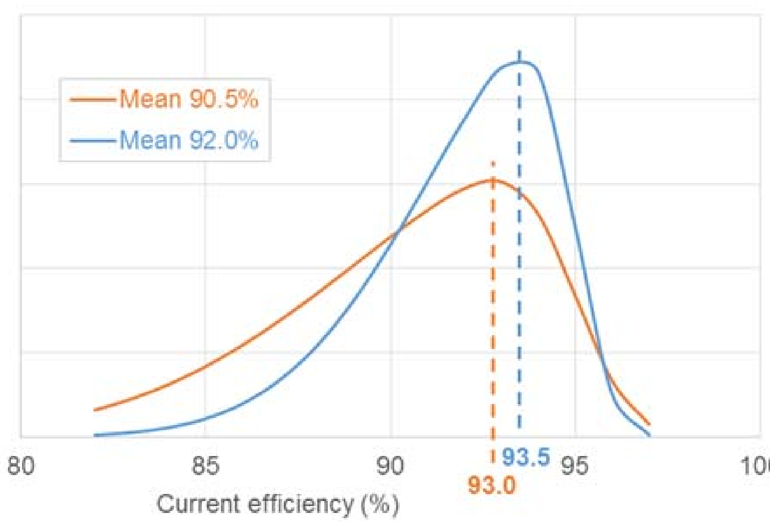


**Figure 4. Illustration of current efficiency distribution within two pot populations.**

## 3. Carbon crisis

### 3.1. Documented case study

The conjunction of anode quality loss and faulty operation may develop into a crisis characterized by high dusting level, overheated cells and lowered production figures. The economic impact may be considerable since crises affect entire potlines. Typical triggers for carbon crises are [10]:

- Poor coke quality (low density, high content of catalytic elements)
- Higher dirty butts fraction
- Recycling of burn-off anodes
- Longer anode cycle
- Poor rodding
- Current creep

If measures are not taken rapidly to act again the triggering causes and to cure the affected pots, the situation can get durably out of hand as a result of the vicious circle described above. In Figure 5, the evolution of carbon content in secondary alumina, bath temperature, current efficiency and number of skimming actions during a documented crisis is plotted. The crisis peak intensity is reached after two months (peak of carbon content in secondary alumina is delayed) and full recovery is achieved six to eight months after the crisis start. The loss in current efficiency attains 2 % and is equal to 1 % in average over six months. One notes that the maximum plant response (skimming actions) occurs in the third month. Not all data was obtainable □ in particular metal production and net carbon consumption are lacking - so that a comprehensive assessment of the income loss was not possible.

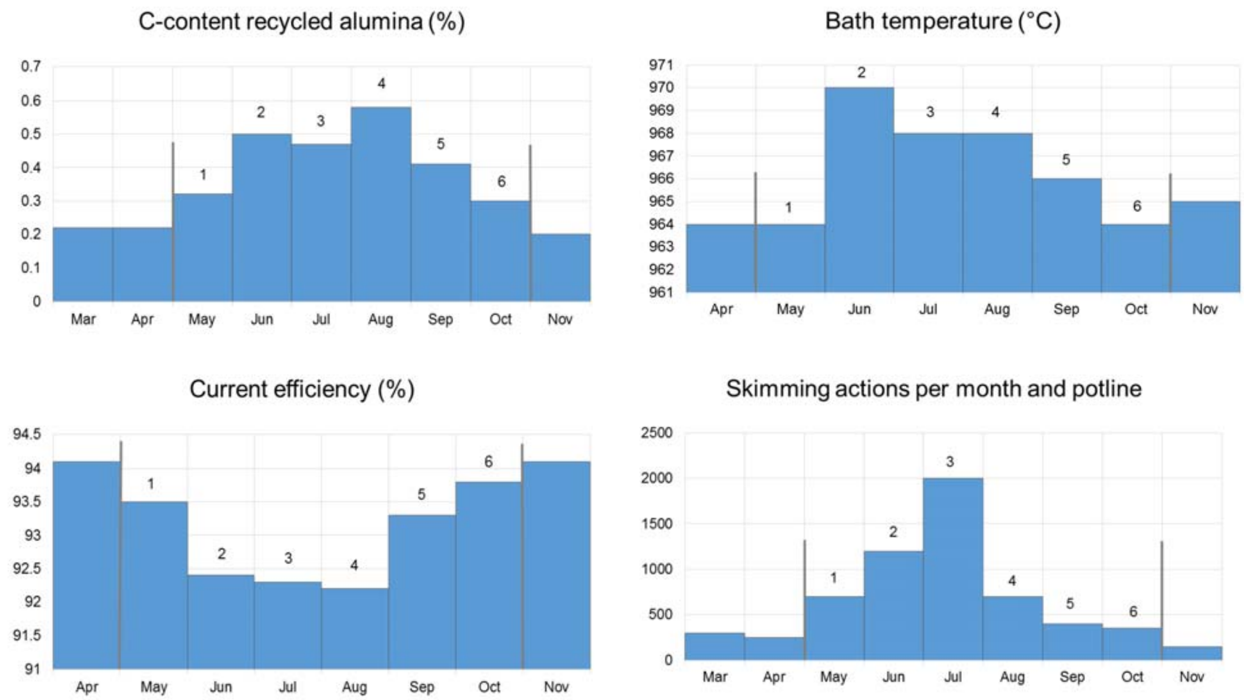


**Figure 5. Evolution of the carbon content in secondary alumina, of bath temperature, of current efficiency and of the number of skimming actions during a documented carbon crisis.**

### 3.2. Economic analysis of virtual crisis scenario

In the following, based on a series of documented carbon crises, a virtual scenario is depicted and its economic impact is analyzed. In Table 2, plant figures are introduced and in Table 3, design target, crisis trigger and crisis partial recover values of anode and pot parameters are listed.

The example of a plant with two potlines, 720 pots operated at 400 kA is taken. Under constant pot operation (pot amperage, bath temperature, anode cycle time), both anode properties and practices (anode setting, rodding, stub reparation, anode cover) are responsible for the propensity to dusting. Regarding anode properties, not only the mean values are relevant but also their variability is since a batch of poor quality anodes generates carbon dust more than proportionally in comparison to standard anodes.

The stub to anode and anode voltage drop values are important in the perspective of energy consumption but also determine anode and bath temperatures with enhancing effect on dusting. They increase from 100 to 150 mV and from 200 to 215 mV in the crisis scenario, influenced by anode rodding and anode resistivity.

**Table 2. Plant figures.**

| SMELTER DESIGN | Unit | |
|---|---|---|
| Potlines | - | 2 |
| Total pots installed | - | 720 |
| Total pots working | - | 716 |
| Pot amperage | kA | 400 |
| Number of anodes | per pot | 48 |
| Current density | $A/cm^2$ | 0.8 |
| Pot voltage target | V | 4.0 |
| Current efficiency | % | 95.0 |
| Sp. energy consumption | MWh/t | 12.55 |
| Metal production | tpy | 800'000 |

Anodic current distribution plays an important role with respect to energy consumption, current efficiency and cell stability. Poor anode balance contributes to dusting via higher anode and bath temperatures, lower current efficiency and more frequent anode incidents. Target is below 10% but it is often measured around 20% due to poor anode setting, variable anode properties and butts size.

The squeeze in ACD resulting from higher stub to anode voltage drop and bath resistivity is well illustrated by the scenarios in Table 2. It is difficult to identify for the operators since only secondary effects are observable/measurable (see Figure 1).

Butts properties and carbon consumption figures are related to both anode quality and pot operation and provide useful information on potential improvements. 50 kg/tAl difference is typically observed between clean pots and pots experiencing a crisis.

In Table 4, the economic consequences of the carbon crisis are detailed. The aluminium production drops as a result of the current efficiency loss. The amount of alumina needed decreases accordingly whereas the anode production (in tons) is reduced due to lower anode density and constant anode cycle time. As a consequence of lower anode density and enhanced net carbon consumption, the butts return is diminished and the amount of coke needed is increased.

In the scenario of a six months crisis with a partial recover during the three last months, the cumulated loss for the plant attains 24 million USD. This will be only the case if measures are taken rapidly after the first signs of deterioration of pot conditions are identified. Even though appropriate actions are specific to the plant and to the root causes, typical measures are:

- Increase of skimming actions,
- Reduction of anode cycle time,
- Increase of anode height,
- Increase of cell voltage,
- Decrease of current.

**Table 3. Design target, crisis trigger and crisis partial recover values of anode and pot parameters.**

| ANODE PROPERTIES | | DESIGN TARGET | | CRISIS TRIGGER | | CRISIS PARTIAL RECOVER |
|---|---|---|---|---|---|---|
| | Unit | Mean | 2σ | Mean | 2σ | Mean |
| Bulk apparent density | kg/dm$^3$ | 1.60 | 0.02 | 1.56 | 0.06 | |
| Sp. electrical resistivity | μΩ·m | 52 | 2 | 58 | 6 | |
| Thermal conductivity | W/(m·K) | 4.5 | 0.5 | 3.5 | 1.0 | |
| Air permeability | nPm | 0.5 | 0.5 | 1.0 | 1.0 | |
| $CO_2$ reactivity residue | % | 90 | 3 | 85 | 8 | |
| $CO_2$ reactivity dust | % | 1 | 1 | 4 | 4 | |
| Air reactivity residue | % | 85 | 5 | 75 | 10 | |
| Air reactivity dust | % | 2 | 2 | 5 | 5 | |
| **OPERATIONS AND ANODE USAGE** | | | | | | |
| Stub to anode voltage drop | mV | 100 | 10 | 150 | 40 | |
| Difference to butts height | mm | 15 | 2 | 17 | 5 | |
| Cover material collapse | % | 2 | | 25 | | |
| Skimming actions | -/pot week | 0.25 | | 0.25 | | |
| Anode cycle time | shifts | 84 | | 84 | | |
| **POT TARGET AND RESULTS** | | | | | | |
| Pot voltage target | mV | 4000 | | 4000 | | 4100 |
| Anode voltage drop | mV | 200 | | 215 | | 215 |
| Bath voltage drop | mV | 1400 | | 1335 | | 1435 |
| ACD voltage gradient | mV/mm | 40 | | 50 | | 45 |
| ACD | mm | 35 | | 27 | | 32 |
| STD anodic current distr. | % | 8 | | 20 | | 15 |
| Noise | mV | 10 | | 40 | | 20 |
| Bath temperature | °C | 950 | | 965 | | 955 |
| C in bath | % | 0.02 | | 0.10 | | 0.06 |
| C in alumina | % | 0.15 | | 0.35 | | 0.25 |
| CE | % | 95 | | 90 | | 93 |
| Sp. energy consumption | MWh/t | 12.55 | | 13.25 | | 13.15 |
| **ANODE AND BUTTS** | | | | | | |
| Butts hardness | mm | 2 | | 6 | | 4 |
| Butts residual section | % | 90 | | 75 | | 85 |
| Butts weight | kg | 290 | | 230 | | 288 |
| Carbon under stub | mm | 25 | | 10 | | 20 |
| Gross carbon consumption | kg/tAl | 560 | | 576 | | 582 |
| Net carbon consumption | kg/tAl | 390 | | 440 | | 410 |
| Butts return | kg/tAl | 170 | | 136 | | 172 |

**Table 4. Economic results.**

| ECONOMICAL RESULTS | Sp. value | Unit | DESIGN TARGET | CRISIS TRIGGER | CRISIS PARTIAL RECOVER |
|---|---|---|---|---|---|
| Al production | | tpy | 800'000 | 758'000 | 783'000 |
| El. energy consumption | | GWh | 10'040 | 10'040 | 10'300 |
| Anode Production | | tpy | 448'000 | 436'600 | 455'700 |
| Butts return | | tpy | 136'000 | 103'000 | 134'600 |
| Coke needed | | tpy | 267'200 | 289'900 | 275'530 |
| Alumina needed | | tpy | 1'552'000 | 1'470'000 | 1'519'000 |
| Loss of Al | | tpy | 0 | 42'000 | 17'000 |
| Loss due to less Al | 1'800 USD/t | Mio USD | 0 | 76 | 31 |
| Extra el. energy | | GWh | 0 | 0 | 260 |
| Loss due to extra el. energy | 40'000 USD/GWh | Mio USD | 0 | 0 | 10 |
| Extra coke needed | | tpy | 0 | 22'700 | 8'330 |
| Loss due to extra coke needed | 400 USD/t | Mio USD | 0 | 9 | 3 |
| Alumina difference needed | | tpy | 0 | -82'000 | -33'000 |
| Savings due to alumina needed | 250 USD/t | Mio USD | 0 | -22 | -8 |
| **Total yearly loss** | | **Mio USD/y** | **0** | **63** | **36** |
| **Total monthly loss** | | **Mio USD/m** | **0** | **5** | **3** |
| **Sp. loss on design capacity** | | **USD/t Al** | | **80** | **45** |

## 4. Conclusions

Maintaining a low and steady concentration of carbon dust in the electrolyte bath is a difficult task. It requires careful selection of raw materials and know-how in the manufacturing and rodding of anodes. At operation level, thermally balanced pots, low bath temperatures and uniform anode current distribution reduce the risk of dusting. The optimal cost/benefit ratio in terms of raw materials, process optimization and anode cycle time shall be determined. In this perspective, an objective assessment of the costs generated by anode dusting shall be realized. Under enhanced stress - current creep to increase Al production, ACD squeeze to limit specific energy consumption, change in anode recipe - pots shall react very differently depending on carbon dust concentration and stability margin. As shown by squeezing tests, the actual ACD may vary by 30 % due to higher bath resistivity. A comprehensive monitoring of anode quality, carbon dust concentration, anode butt properties plays an integral part in the prevention of carbon crises.

## 5. References

1. Grjotheim K., Krohn C., Thonstad J., Einige offene Fragen bei der heutigen Aluminiumelektrolyse, 5. Internationale Leichmetalltagung 1968, pp 343-346.
2. Foosnæs T., Naterstad T., Bruheim M., Grjotheim K., Anode dusting in Hall-Héroult cells, Light Metals 1986, pp 633-642.
3. Meirbekova R., Haarberg G. M., Thonstad J., Ziegler D. P., Brynjarsson J., Saevarsdottir G., Effect of operational parameters on the behavior of phosphorus and sulfur in aluminum reduction, Light Metals 2015, pp 559-564.
4. Tordai T., Anode dusting during the electrolytic production of aluminium, Thesis #3808, Ecole polytechnique fédérale de Lausanne, 2007.

5. Fischer W. K., Perruchoud R. C., Factors influencing the carboxy- and air- reactivity behaviour of prebaked anodes in Hall-Héroult cells, Light Metals 1986, pp 575-586.
6. Gudmundsson H., Anode dusting from a potroom perspective at Nordural and correlation with anode properties, Light Metals 2011, pp 471-476.
7. Vetyukov M. M., Chuvilyaev R.G., Izv. Vyssh. Ucheb. Zaved., Tsvet Met. 7(6), 74, 1964.
8. Tarcy G. P., Tørklep K., Current efficiency in prebake and Søderberg cells, Light Metals 2005, pp 319-324.
9. Híveš J., Thonstad J., Sterten Å., Fellner P., Light Metals 1994, pp 187-194.
10. Perruchoud R. C., Hulse K. L., Fischer W. K., Dust generation and accumulation for changing anode quality and cell parameters, Light Metals 1999, pp 649-656.